Biostratigraphic investigations assisted by virtual outcrop modeling: a case study from an Eocene shallow-water carbonate succession (Val Rosandra gorge, Trieste, NE Italy)

Lorenzo Consorti[1], Amerigo Corradetti[2], Mehdi Hadi[3], Marco Franceschi[2], Monia Sabbatino[2], Sara Bensi[4], Nicolò Bertone[2] & Lorenzo Bonini[2]

[1] Istituto di Scienze Marine (ISMAR-CNR), Area Science Park, Basovizza, Trieste, Italy.

[2] Dipartimento di Matematica, Informatica e Geoscienze, Università di Trieste, Via Weiss 2, Trieste, Italy.

[3] Independent Researcher in Stratigraphy and Paleontology, Mashhad, Iran.

[4] Direzione centrale difesa dell'ambiente, energia e sviluppo sostenibile, Servizio geologico, Regione Friuli Venezia Giulia, Via Sant'Anastasio 3, Trieste, Italy.

LC, 0000-0001-9544-3960; AC, 0000-0002-5174-0653; MH, 0000-0001-6082-4552; MF, 0000-0002-2061-0151; MS, 0000-0002-4693-1631; NB, 0000-0002-8428-9643; LB, 0000-0001-5613-7813.

Ital. J. Geosci., Vol. 143, No. 1 (2024), pp. 60-74, 10 figs., https://doi.org/10.3301/IJG.2024.04.

Research article

Corresponding author e-mail: amerigo.corradetti@units.it

Citation: Consorti L., Corradetti A., Hadi M., Franceschi M., Sabbatino M., Bensi S., Bertone N. & Bonini L. (2024) - Biostratigraphic investigations assisted by virtual outcrop modeling: a case study from an Eocene shallow-water carbonate succession (Val Rosandra gorge, Trieste, NE Italy). Ital. J. Geosci., 143(1), 60-74, https://doi.org/10.3301/IJG.2024.04.

Associate Editor: Domenico Cosentino

Guest Editor: Chiara Zuffetti

Submitted: 29 March 2023

Accepted: 28 October 2023

Published online: 06 December 2023

SUPPLEMENTARY MATERIAL is available at: https://doi.org/10.3301/IJG.2024.04

SOCIETÀ GEOLOGICA ITALIANA
FONDATA NEL 1881 - ENTE MORALE R. D. 17 OTTOBRE 1885

ISPRA
Istituto Superiore per la Protezione e la Ricerca Ambientale

Sistema Nazionale per la Protezione dell'Ambiente

ABSTRACT

Virtual outcrop modeling has emerged as a tool for supporting geological field activities such as geological mapping and stratigraphic investigations. Here we show how this technique can be used to support the detailed stratigraphic logging and sampling with a case history from the Eocene carbonate platform succession exposed in the Val Rosandra gorge, in the vicinity of the city of Trieste, NE Italy. The biostratigraphic analysis highlighted the occurrence of Shallow Benthic zones (SBZ) 10 to 12 and the planktonic zones E7/E8. An upwards-deepening trend, from inner platform to a hemipelagic domain, is observed through the studied stratigraphic interval and is in accordance with the vertical evolution recorded in other Eocene successions of the Adriatic Carbonate Platform. Aerial drone imaging was used to produce a virtual outcrop model of the studied succession that provided a high-resolution geometrical framework for field measurements, sample geotagging and observations. For instance, the virtual outcrop model assisted in determining the true thickness of beds, a task that can be subject to significant imprecisions when measurements are taken by hand. Ultimately, the integration of virtual outcrop modeling with classical sampling and measuring methods resulted in accurate stratimetry and in the precise spatial positioning of samples that were taken for biostratigraphy and facies characterization.

KEY-WORDS: CARG project, Carbonate platform, *Alveolina*, Biostratigraphy, 3D model, Orthoimages.

INTRODUCTION

Paleogene shallow-water successions are widespread throughout the peri-Mediterranean area and consist of lithified marine sediments rich in larger Foraminifera, corals, and red algae (e.g., Pignatti, 1995; Ćosović et al., 2004; Scheibner & Speijer, 2008). Such depositional environments have been interpreted as carbonate ramps (Accordi et al., 1998; Vecsei et al., 1999; Ćosović et al., 2018; Briguglio et al., 2023). Key biological and climate events, such as the benthic aftermath of the Cretaceous-Paleocene (K-Pg) mass extinction and the hyperthermal event at the Paleocene-Eocene boundary (PETM; see Zamagni et al., 2012) are recorded along. A great diversity for larger Foraminifera is observed already soon after the K-Pg (Drobne et al., 2014; Sinanoğlu et al., 2022) and throughout the whole Paleocene and Eocene (Hottinger, 2001; Benedetti & Papazzoni, 2022) punctuated by repeated bioevents, used in biostratigraphy for the identification of standard biozones, named Shallow Benthic Zones (Serra-Kiel et al., 1998) that are, for the Paleocene, also calibrated with the calcareous nannofossil biostratigraphic scale (SBP; Papazzoni et al., 2023).

In this paper, we carried out a detailed stratigraphic sampling of the Eocene shallow-water carbonate succession exposed in the Val Rosandra gorge, near Trieste, and included in sheet 110 "Trieste" of the new geological map of Italy released in the frame of the CARG Project (geologic and geothematic cartography of Italy at 1:50,000). The Eocene rocks widely crop out in the gorge, but field conditions make logging at times complex as sections are often of difficult

accessibility because of steep cliffs, complex structural settings and thick vegetation. For this reason, here classical fieldwork is coupled with drone imagery and virtual outcrop modeling to perform accurate logging and samples' geotagging. The advent of three-dimensional virtual outcrop modeling techniques has offered new possibilities to accurately collect data from outcrops (e.g., Marques et al., 2020; Seers et al., 2021). Among the techniques to produce virtual outcrop models, structure from motion–multiview stereo (SfM-MVS) digital photogrammetry (e.g., Arbués et al., 2012; James & Robson, 2012; Favalli et al., 2012; Bemis et al., 2014; Tavani et al., 2014), particularly thanks to the advances in drone imagery, has emerged as a flexible, precise and easy-to-use methodology. This technique has progressively been applied in diverse disciplines including structural geology (Franceschi et al., 2015; Corradetti et al., 2017; Camanni et al., 2021), fracture stratigraphy (Manniello et al., 2023), geomechanics (Menegoni et al., 2019; Furlani et al., 2022; Schilirò et al., 2022; Mammoliti et al., 2023), geomorphology (Brodu & Lague, 2012; Carrivick & Smith, 2019; Devoto et al., 2020) stratigraphy (Nesbit et al., 2018) and sedimentology (Fabuel-Perez et al., 2010; Jablonska et al., 2021) among many others.

Stratigraphic sampling in the field and data release are usually framed by sketch drawings/taking pictures at the sample locality, the associated coordinate position of the base of the stratigraphic sections, logging, and, in some cases, granting access to samples. Geological field activities and field data documentation and distribution can be significantly improved where the work is supported by 3D digital modeling techniques as they may allow, for instance, accurate positioning of measurements/observations, imaging of areas that are of difficult accessibility, identification of the best sampling path, digital documentation of the examined outcrop through time.

The objective of this study is threefold: (i) demonstrate the potential advantages offered by the integration of virtual outcrop modeling in stratigraphic investigations; (ii) build a potential reference section for the Eocene lithostratigraphic unit outcropping in the area which is included in the sheet 110 (Trieste) of the CARG project; (iii) provide a detailed biostratigraphic frame of the sampled section by applying SBZs, mostly based on the vertical range of species of the foraminiferal genera *Alveolina*, and, secondarily, on plankton biozonation for the hemipelagic portion.

The present paper provides a brief and comprehensive contribution to the use of drone imagery as support in classic stratigraphic fieldwork. We discuss the implications of using drones during fieldwork and the potential advantages of having a virtual outcrop model at hand when constructing a stratigraphic section and studying an outcrop. Moreover, results of biostratigraphic and facies investigations allow framing the studied succession within the general evolution of the Adriatic Carbonate Platform during the Eocene.

Finally, the application of 3D virtual outcrop modeling techniques provides quantitative information (e.g., the trace of the sampled section, the position of each sample, and the bedding attitude) that could potentially be used to enrich the CARG project digital database.

GEOLOGICAL SETTING AND STRATIGRAPHY

The studied outcrop is located in the municipality of San Dorligo della Valle/Dolina, near the city of Trieste (Italy) and next to the Slovenian border where the Rosandra Gorge originates (Fig. 1). From the structural point of view, the area belongs to the northwestern sector of the External Dinarides (e.g., Otoničar, 2007). The latter is a fold-and-thrust belt formed during the NE-SW-oriented Jurassic-Eocene convergence between the European and Adria-related units (Schmid et al., 2008; van Unen et al., 2019; van Hinsbergen et al., 2020). In this region, the most obvious result of such convergence is the iconic Kras-Carso plateau, made of rocks belonging to the Adriatic Carbonate Platform (AdCP; "*sensu lato*" in Korbar, 2009; Vlahović et al., 2005; Jurkovšek et al., 2016; Consorti et al., 2021), which extends in a northwest–southeast direction (Fig. 1b). During the Mesozoic, the Kras-Carso was situated at the NW side of the wider AdCP that was part of the peri-Adriatic Mediterranean archipelago composed of isolated carbonate shelves bordered by deep basins. The shallow-water carbonate succession of the Kras-Carso plateau is composed of a thick pile (up to 1.5 km) of Mesozoic to lower Eocene shallow-water carbonates – mainly limestone and, in minor proportions, dolostone and breccia, and a middle Eocene siliciclastic succession containing sparse carbonate olistoliths (Jurkovšek et al., 2016). The lithostratigraphy of these Meso-Cenozoic units has been proposed by several Authors, to which we refer for further reading (e.g., Cucchi et al., 1987; Vlahović et al., 2005; Korbar, 2009; Jurkovšek et al., 2016; Consorti et al., 2021). The studied section encompasses the upper part of the "miliolids, *Alveolina* and *Nummulites* limestone" *sensu* Consorti et al. (2021), referable to the "Alveolinid-Nummulitid limestone" of Jurkovšek et al. (2016), or "Foraminiferal limestone" of Vlahović et al. (2005) and Korbar (2009), which age spans, in the Kras-Carso, through the mid Paleocene and the early Eocene. The Eocene successions of the AdCP can be also found in the subsurface of the Friuli region (there called Friuli Platform), in Slovenia and along the coast of Croatia, in Bosnia and Montenegro (Drobne et al., 2011; Ibrahimpašić et al., 2015; Ćosović et al., 2018, among others). The drowning of the Eocene carbonate succession is characterised by hemipelagic limestone facies containing planktonic Foraminifera like *Acarinina, Subbotina* (see Ibrahimpašić et al., 2015). This is followed by a thick succession of foredeep siliciclastic deposits, referred to in the literature as "Transitional beds", "Flysch" or "Promina deposits", among other terms. These deposits may span from the middle Eocene to the Oligocene, indicating basin evolution associated with the Dinarid orogeny (Tari Kovačić and Mrinjek, 1994; Korbar, 2009).

MATERIALS AND METHODS

The fieldwork was carried out in early October 2022. Logging and sampling were made working on the outcrops located on the northern flank of the gorge. (Fig. 2a and b). On the southern side of the gorge, from a panoramic point of view, visual support was provided and an aerial photo acquisition of the section was carried out by means of an Uncrewed Aerial Vehicle (UAV) device, aka a drone. The two teams were in radio contact (Fig. 2a).

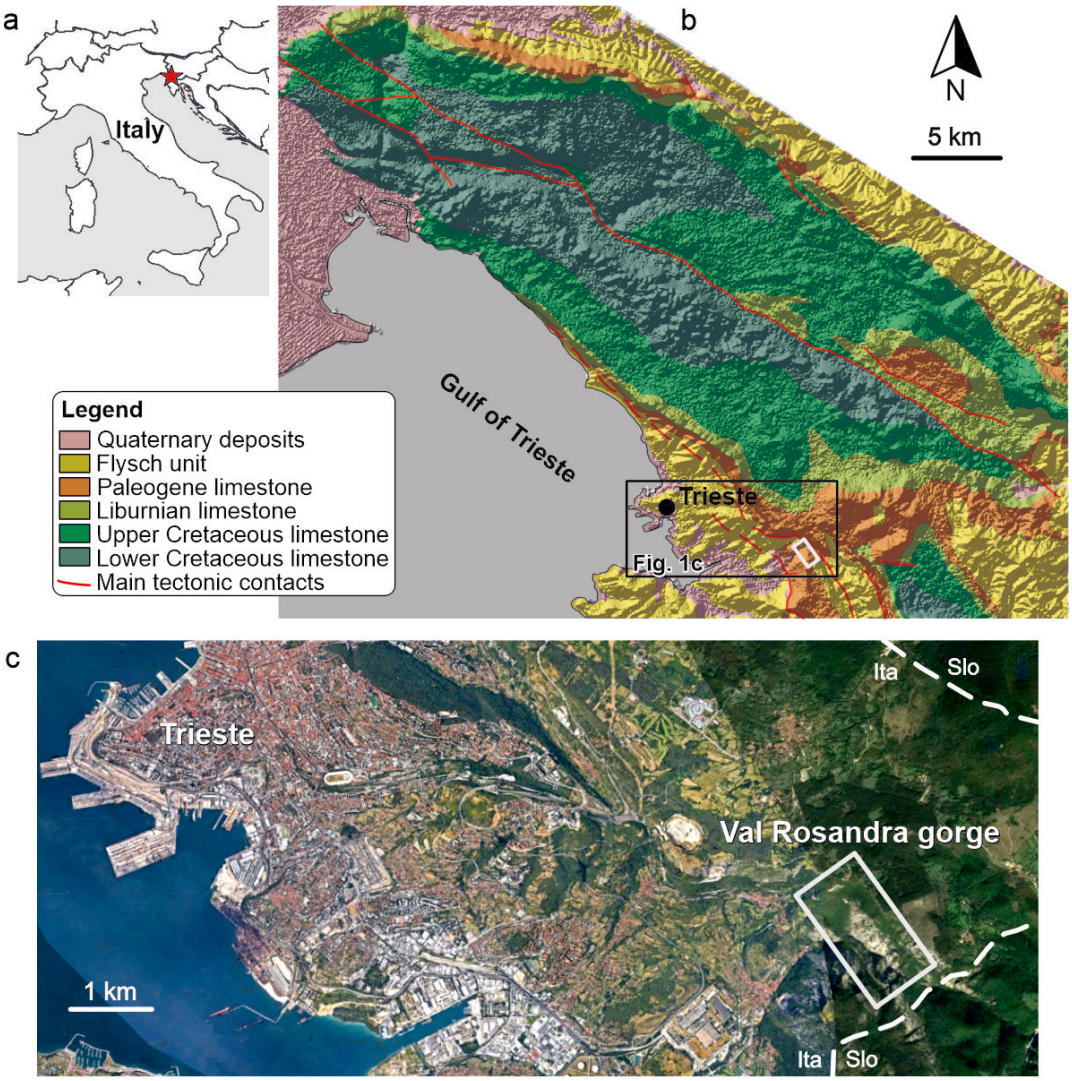

Fig. 1 - (a) Map of Italy with the position of the studied area (red star). (b) Simplified geological map of the Karst Region, simplified from Jurkovšek et alii (2016). (c) Position of the Val Rosandra gorge within the Trieste municipality (taken from Google Earth).

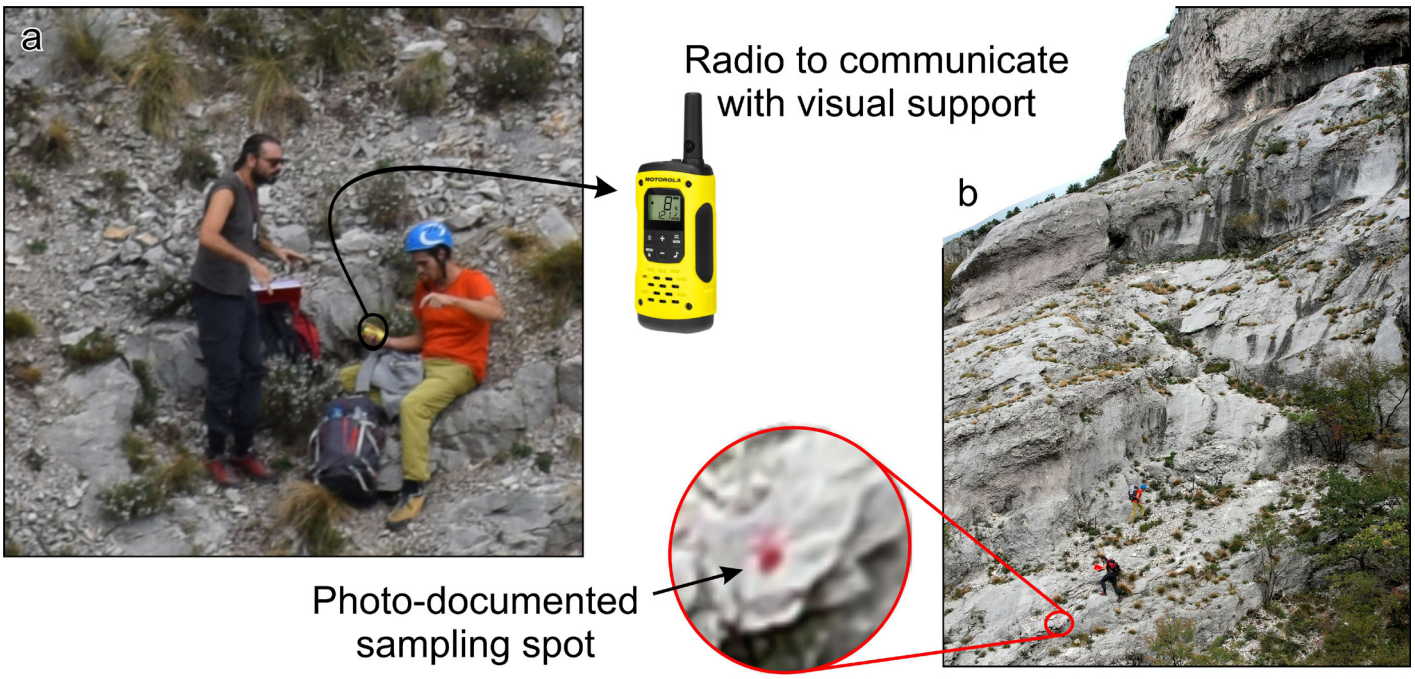

Fig. 2 - Images collected during the visual support to the team sampling the stratigraphic column. The two teams were in radio contact (a). (b) Image showing one of the stratigraphic sampling positions that was marked with a red dot on the outcrop.

Field data acquisition and analysis

Equipped with the traditional tools of field geologists (hammer, lens, ruler, and notebook), the first team started sampling the succession from the lower portion of the gully up to the cyclable-pedestrian track along the former Trieste-Erpelle railway track. Limestone samples (labeled VR-) were collected by walking straight across the beds to build the reference stratigraphic column, samples were taken with a spacing of about 1 to 2 metres; a total of 73 samples were collected along the stratigraphic column. Additional 20 scattered foraminiferal-rich limestone samples (labeled AC-) were collected from the northern side of the gorge and surrounding areas. Thin sections and polished slabs were prepared from the samples; facies were defined in terms of texture, components and palaeoenvironmental meaning according to Flügel (2010) and Ćosović et al. (2004; 2018) for specific reference to the Paleogene of the AdCP. Samples' foraminiferal content was photographed with a microscope digital camera using both transmitted and reflected light, whereas we used (mostly but not exclusively) Hottinger (1974), Serra-Kiel et al. (1998), Drobne et al. (2009; 2011) and Ibrahimpašić et al. (2015) for taxonomic discriminations and biostratigraphy.

Due to the mentioned difficult accessibility and vegetation and debris cover, the logging and sampling were carried out following discrete paths, with the aim of then merging collected data together as a composite section into a synthetic stratigraphic column. Constant radio support was hence necessary to guide the team during the work. The support team provided guidance to choose the path in order to guarantee continuous composite sampling.

Drone imaging and visual support

The drone used for the photo acquisition is a DJI Air 2S. This model has an embedded GNSS positioning system (GPS, GLONASS, and Galileo constellations), a compass, and an inertial measurement unit (IMU) allowing a hovering accuracy range of vertical and horizontal positioning with GNSS of ~0.5 m and ~1.5 m respectively. The DJI Air 2S has a 20-megapixel camera with a 1" CMOS sensor, mounted on a three-axis gimbal. A total of 658 photos were collected in JPG format (5472 × 3648 pixels) in manual flight mode, prioritizing image overlap along the sampling path (Fig. 3a). The lens angle of view is 22 mm (35 mm equivalent).

While guiding the team working along the section and operating the drone, the support team was kept up to date with the sampling tag number so that, with the help of an iPad Pro, the position of the samples was noted over panoramic photographs of the cliff. Every now and then, the stratigraphic sampling position was marked with a red dot on the rock (Fig. 2b), which was promptly photographed from the drone or using a Single Lens Reflex (SLR) with a telephoto lens to preserve drone batteries. This documentation made by the support team was very important since the accurate geotag of the samples could not be resolved by the team in charge of the sampling using a handheld GNSS receiver. Indeed, a handheld GNSS receiver, like, for example, a smartphone, would not be resolutive enough on this very steep cliff since a small horizontal position uncertainty may lead to a very large vertical error.

3D virtual outcrop model construction and identification of sampling spots

The aerial photographs were processed in Agisoft Metashape software to build the virtual outcrop model of the northern side of the Val Rosandra gully. The well-known workflow of Metashape (Verhoeven, 2011; Tavani et al., 2014; Carrivick et al., 2016) involved the high-accuracy alignment of the photographs followed by an iterative gradual selection filtering and camera optimization steps leading to a final Tie-Point cloud made of ~3M points (Fig. 3a). The medium-quality densification returned a dense cloud made of ~54M points that were also filtered based on point confidence (Fig. 3b). The resulting mesh was computed at 8M faces (Fig. 3c) and textured (Fig. 3d). A tiled model was also generated to improve graphic resolution within Metashape. A smaller, high-confidence portion (Fig. 3c) of the modeled area, which includes the sampled section, was selected and retextured (Fig. 3e). Scaling and georeferencing of the model were granted by the image geotags acquired through the drone GNSS sensor. Typically, drones like the DJI Air 2S, when served by appropriate satellite coverage, have a few metres of error in position accuracy and high precision (Corradetti et al., 2022). This accuracy error can be considered negligible when the cameras' positions are distributed over several hundreds of metres (Fig. 3a) (e.g., Menegoni et al., 2019; Panara et al., 2022). Larger errors typically resolve into very minor rigid translations in the latitude-longitude components that may become not negligible in the vertical component (Corradetti et al., 2022). Therefore, the Val Rosandra gorge model can be considered accurate enough with respect to its orientation and internal scale for the purpose of this work.

Since not all of the sampling spots were marked on the outcrop, their identification in Metashape occurred in two phases. First, all marked spots were identified in the model from the aligned images (Fig. 4a). In essence, the spots were identified from the images and Metashape repositioned them in the 3D space (Fig. 4b). The sampling spots that were not marked were positioned thanks to photographs and notes taken on the iPad from the visual supporting team with assistance from the surveyors who carried out the sampling. This procedure allowed identifying all the sampling spots in the 3D model (Fig. 3e; 4c).

The high-confidence 3D model of the northern side of the Val Rosandra gully (Fig. 3e) was exported for structural investigation. A lower-resolution version of the larger model (Fig. 3d) has been made available in public repositories like Sketchfab (https://skfb.ly/oyN6E) and V3Geo (Buckley et al., 2022) (https://v3geo.com/model/452). The aerial imagery also enabled the production of a high-resolution aerial orthoimage of the area, which can help the geological mapping. Unfortunately, the free basic subscription in Sketchfab does not allow annotations of more than 10 points, so we decided to only tag the beginning and end of the stratigraphic section in the model stored in Sketchfab. Likewise, V3Geo does not yet implement a shareable interpretation tool which is instead provided through the commercial software LIME (Buckley et al., 2019). Two *.kmz files providing sampled traces and sampled spots to be viewed on Google Earth are provided as supplementary material (Supplement 1 and Supplement 2). Note that mismatches

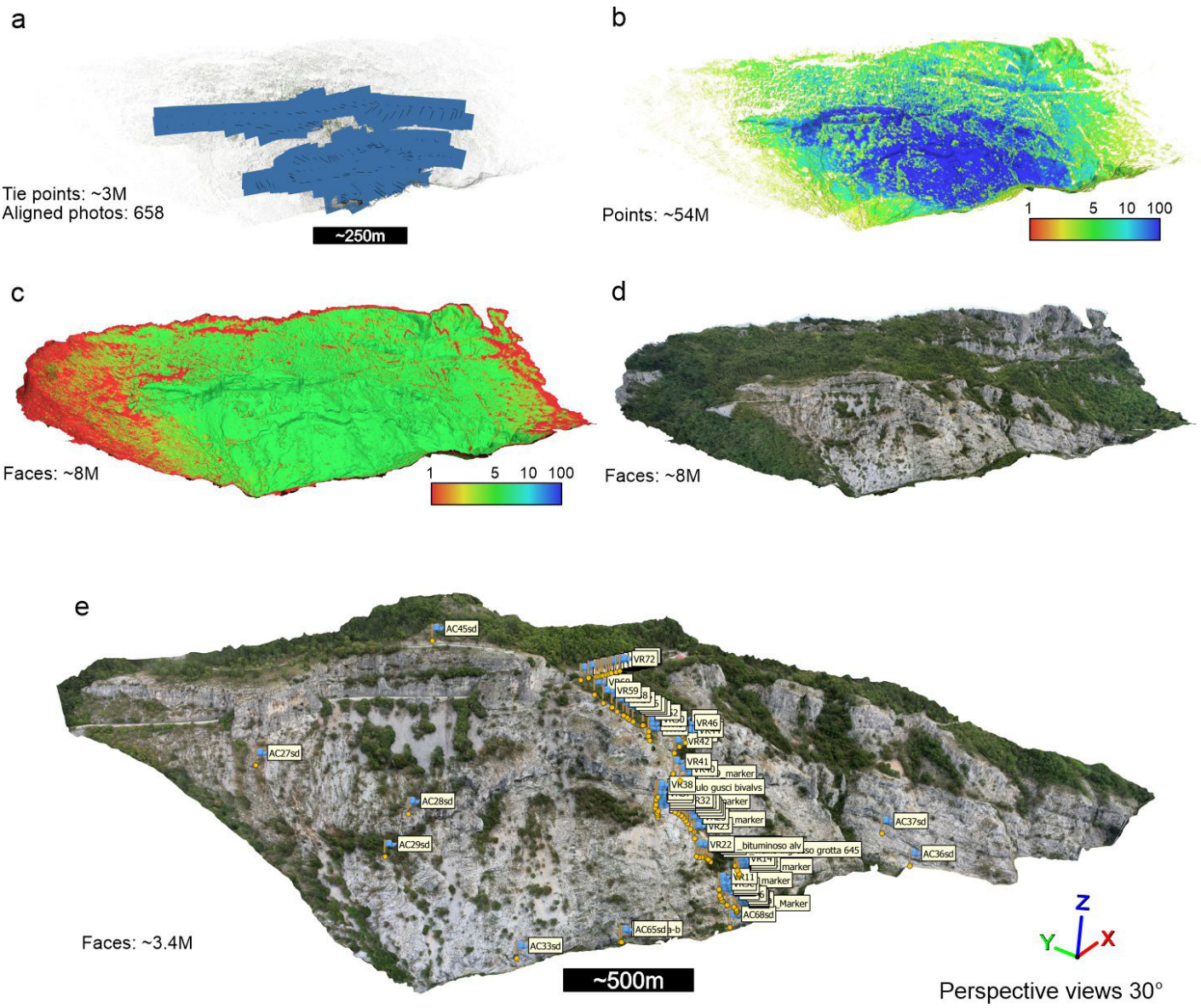

Fig. 3 - Perspective views of the northern side of the Val Rosandra gully. (a) Tie-points cloud with camera positions. (b) Filtered-dense cloud coloured by point confidence assigned by Metashape. (c) Mesh model with faces coloured by confidence assigned by Metashape; note that red faces correspond to extrapolated areas from the dense cloud. (d) Textured model with sampling points. (e) High-confidence textured model of the stratigraphic section. Models in a, b, c, and d have the same scale, while all the models (including model e) share the same perspective point of view.

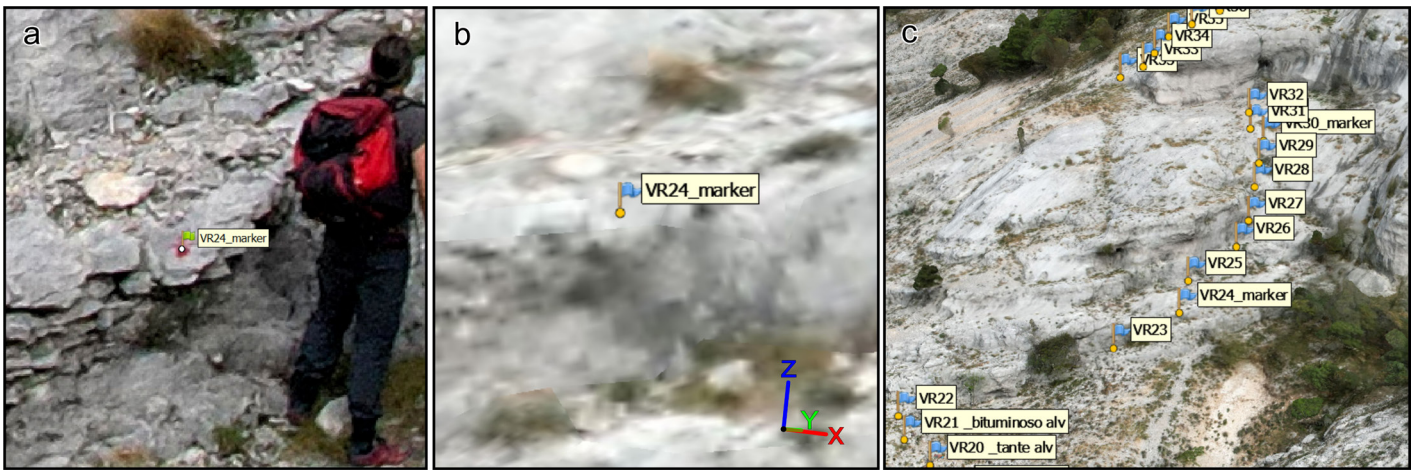

Fig. 4 - (a) Marker identification from aligned photographs in Metashape. (b) One of the markers that was automatically repositioned in the 3D space of Metashape. (c) Some markers corresponding to sampling points repositioned in the model.

exist between the Google Earth elevation model and the higher-resolution 3D model produced in this work from which the traces have been digitalized connecting sampled spots. Moreover, as detailed above, since the model was registered using only the image geotags provided by the drone, the elevations of the sampled spots should not be considered absolute elevations.

Data extraction and model orthorectification

The textured outcrop mesh of the study area (Fig. 3e) was loaded in the recently released version of Openplot free software (v. 1.05; Tavani et al., 2011), where visible and well-expressed geological features were digitized. For details on the technical usage of Openplot readers are referred to available literature (e.g., Tavani et al., 2016; Corradetti et al., 2017). In short, the software uses digitized polylines to calculate best-fit planes in real-time (Fig. 5a), allowing the user to evaluate in 3D whether to reject or retain each plane. This visual evaluation is essential considering that it is a common user error the digitization of polylines that return best-fit planes that follow the outcrop topography rather than the penetrating geometry of the geological planar features of interest (e.g., Fernández et al., 2009; Jones et al., 2016; Seers and Hodgetts, 2016). Bedding planes, fractures, and faults that are well-expressed in the model were digitized (Fig. 5b-c). Bedding plane orientations were used to produce properly oriented orthoimages of the model that have been used to recalculate the bed thickness (e.g., Corradetti et al., 2017; Menegoni et al., 2018; Tavani et al., 2023), and to re-drawn the stratigraphic column as shown in the figure provided in the supplementary material (Supplement 3). In essence, properly oriented orthoimages are perpendicular to bedding photo-realistic cross sections of the 3D model, and thus thicknesses in orthoimages are the most reasonable approximation of stratigraphic thickness. The success of the orthorectification of the model and thus of the beds' thickness calculation from the orthoimages relates to diverse factors. Among them, a major role is played by (i) the internal accuracy of the model (i.e., its scaling and its internal geometrical consistency), (ii) the coplanarity/collinearity factors of the digitized polylines (e.g., Fernández, 2005), and, in the case of folded strata, (iii) to the fold's cylindricity.

RESULTS

Limestone facies and palaeoenvironment

The thickness of the carbonate succession exposed in the Val Rosandra section and measured in the field was estimated in 132 metres. The first 107 metres are made of shallow-water facies. A rough subdivision into facies associations of this stratigraphic portion includes: i) miliolids and *Alveolina* grainstone (in some cases fine-grained) and packstone with subordinate rudstone. Components include other foraminiferal fragments (*Nummulites*, *Orbitolites*, smaller Foraminifera and rotaliids) and corallinacean red algae; ii) packstone to floatstone in which the main components are *Alveolina*, miliolids and other porcelaneous taxa (e.g., *Spirolina* sp.) and subordinate *Nummulites*, with few levels of fine-grained packstone/grainstone with miliolids and *Cibicides* (Fig. 6b). A dominance of porcelaneous taxa suggests deposition in a shallow ramp (Ćosović et al., 2004; Flügel, 2010) of an oligotrophic sea bottom within the photic zone at a very shallow depth (similar to facies MF1 and MF2 of Ćosović et al., 2018 in the AdCP, see also Romero et al., 2002). The characteristic *Alveolina*-rich accumulations (Fig. 6a) indicate indeed high energy above the mean fair-weather wave base, whose deposition is driven by intense winnowing under well-illuminated conditions (facies MF3

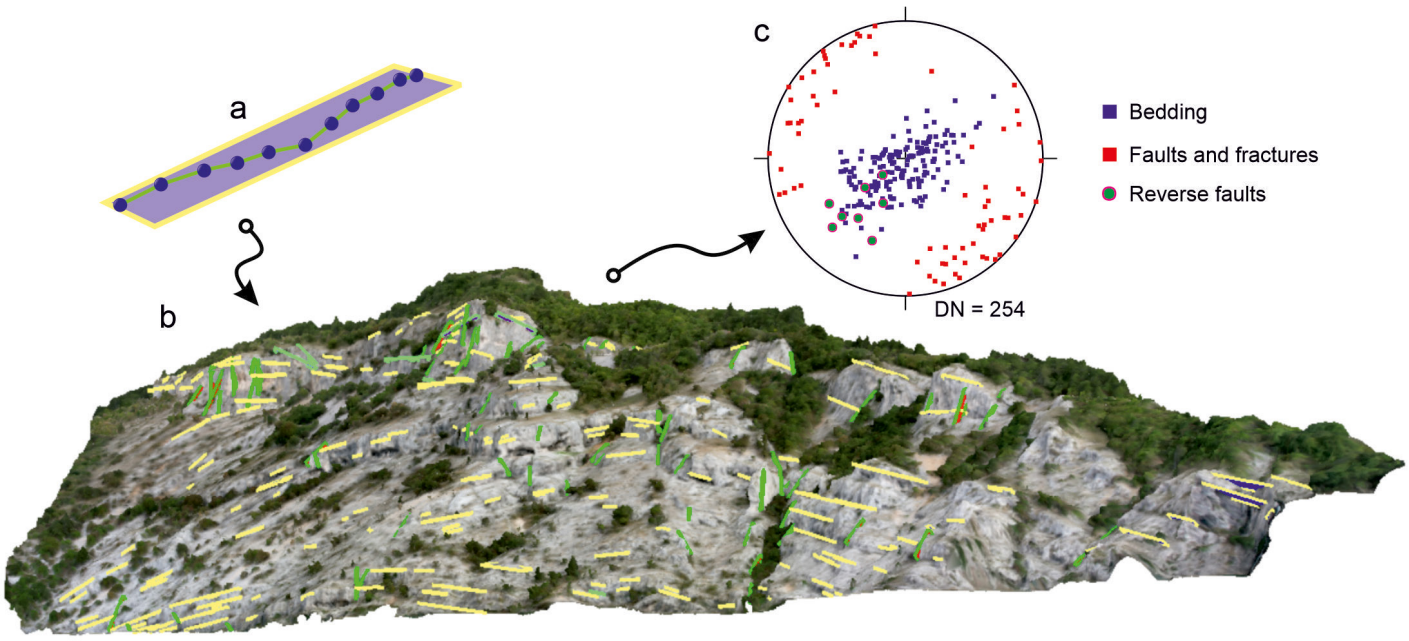

Fig. 5 - (a) Example of a best-fit plane from a polyline. (b) Perspective view (30°) from the South of the virtual outcrop model interpreted in Openplot. Bedding planes are depicted as rectangles with a yellow outline, while faults and fractures have a green outline. (c) Lower hemisphere equal-area projections of poles to bedding and faults. DN is the number of planar features extracted.

of Ćosović et al., 2018). These shallow-water facies alternate in the first 100 m of the section (Fig. 7). In several cases, the matrix of floatstone to packstone appears comparatively darker with traces of organic matter, suggesting proximal position of a restricted environment (e.g., lagoon). This possibly corresponds to the quasi-lagoonal environment of Ćosović et al. (2018) pointing to innermost ramp areas protected from waves by shoals or seagrass meadows. Upward in the section, through the last 25 metres of succession (Fig. 6c), fine-grained packstone with scarce planktonic foraminifera along with *Nummulites-Operculina*-orthophragminid packstone/floatstone with sparse fragments of and corallinacean red algae alternate throughout. Such facies change suggests that the depositional environment shifted to a deeper setting, into the lower photic zone of the mid-outer platform. This is especially denoted by planktonic foraminifera and the abundance of flat lamellar perforated larger foraminifera (Fig 6c). Among the latter, *Operculina*, whose Recent distribution in the water column is precisely constrained by the ecological requirements of algal symbionts hosted in the shell, indicates the lower photic zone (Hottinger et al., 1978,1997; Leutenegger, 1984; Hohenegger, 2000). Planktonic foraminifera become abundant, appearing well-preserved in few levels (see Fig. 7) characterized by fine-grained wackestone facies (Fig. 6d), indicating a hemipelagic environment. The occurrence of the marly "Transitional beds" (*sensu* Jurkovšek et al., 2016) on top of the hemipelagic facies marks the definitive drowning of the carbonate platform and the switch to siliciclastic deposition, testified by the turbidites of the "Trieste Flysch".

Biostratigraphy

In this work, we have focused our attention on the biostratigraphic value of the species contained within the foraminiferal genera *Alveolina*, for correlations with the Shallow Benthic Zones (SBZ) of Serra-Kiel et al. (1998). The SBZs are polytaxic Oppelian biozones defined by the distribution of index larger foraminiferal assemblages (including species of *Nummulites*, orthophragminids and soritids among others) that are anchored to standard stratigraphic scales such as planktonic microfossil and

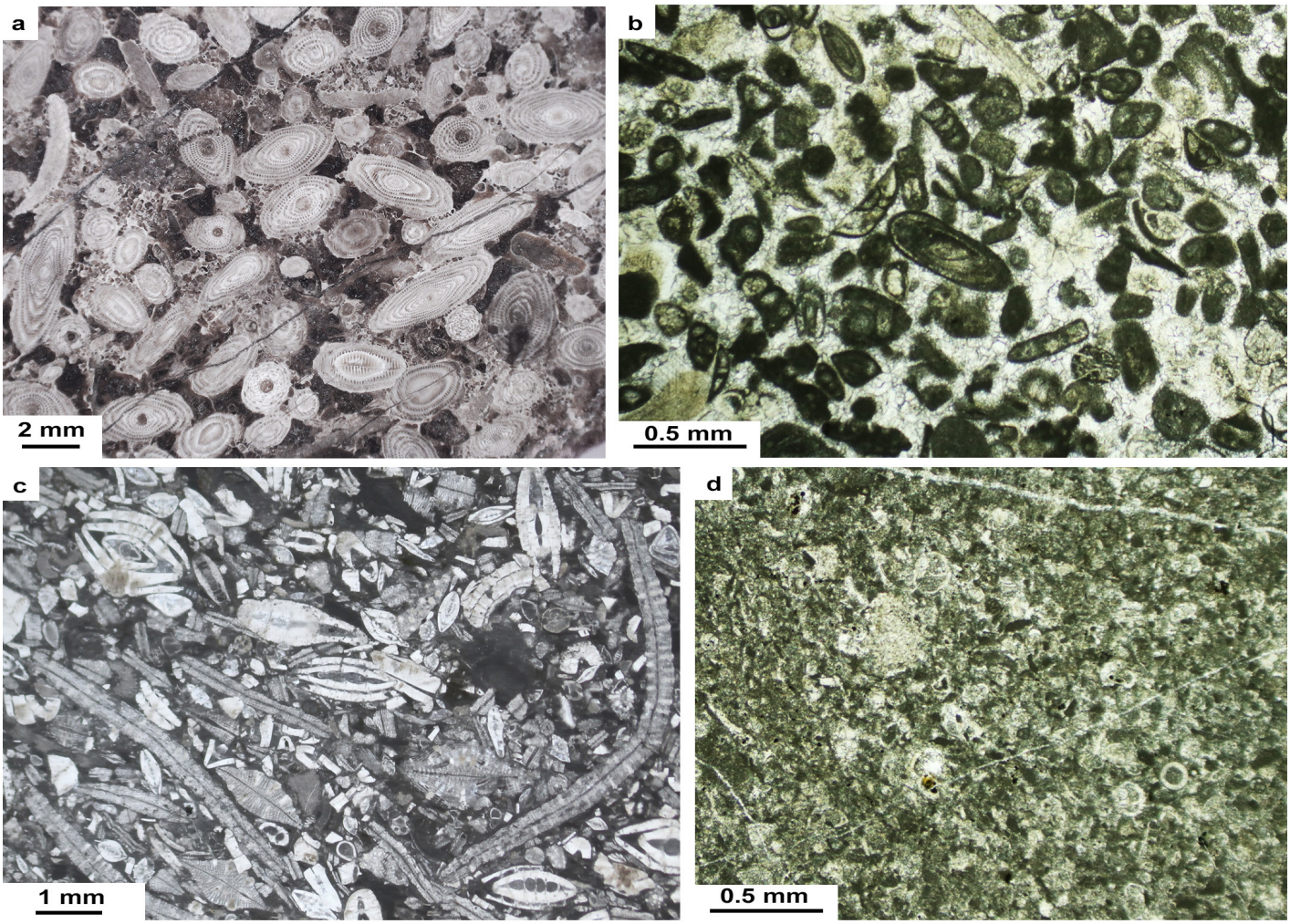

Fig. 6 - Facies examples of the Val Rosandra gorge "miliolid, *Alveolina* and *Nummulites* limestone" unit, from the sampled column. (a) *Alveolina* grainstone deposited as a bioclastic lag in proximal platform setting, polished slab, sample VR9c. (b) Well-sorted fine-grained grainstone of inner platform setting, thin section, sample VR22. (c) *Nummulites-Operculina*-orthophragminid packstone (floatstone) of mid-platform setting, lower photic zone, thin section, sample VR64. (d) Hemipelagic fine-grained wackestone-packstone with planktonic foraminifera, thin section, sample VR70. (a): reflected light; (b-d): transmitted light.

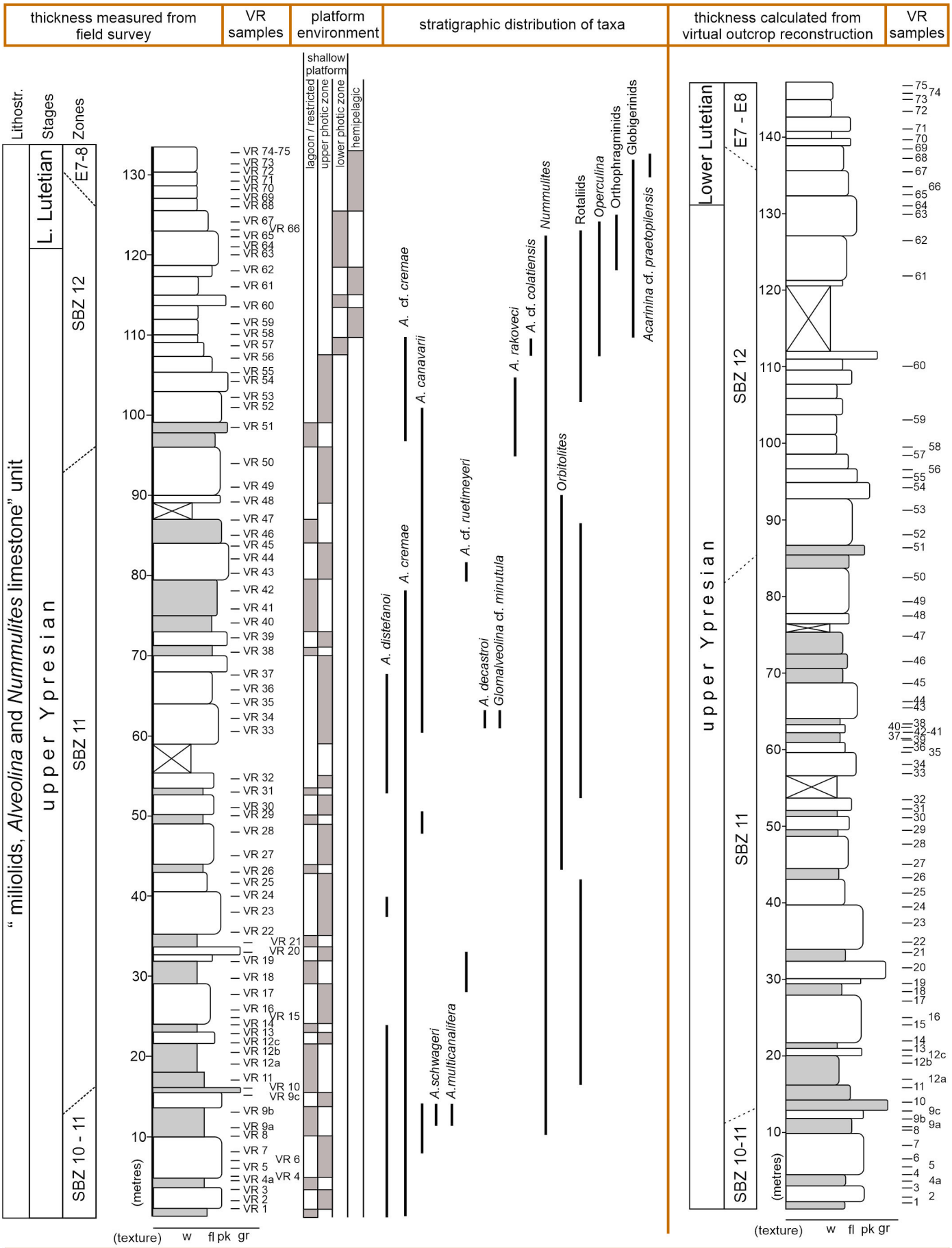

Fig. 7 - Stratigraphic log measured in the field, facies, samples positions and taxa distribution vs. the log redrawn after the virtual outcrop orthorectification. Limestone texture abbreviations: w: wackestone; fl: floatstone; pk: packstone; gr: grainstone. Beds in grey colour indicate organic matter-rich facies.

magnetostratigraphy (Pignatti & Papazzoni, 2017) and therefore with a reliable chronostratigraphic value. The resolution of SBZs extends from W Europe to Tibet, through some discrepancies between far areas of the Neo-Tethyan Ocean exist (Zhang et al., 2013). In the peri-Mediterranean platforms, such as the AdCP, SBZs can be considered fairly reliable (see Drobne et al., 2009, 2011).

The oldest *Alveolina* assemblage (Fig. 8) encountered in the Val Rosandra section is composed of some index markers such as *A. schwageri* Checchia-Rispoli, *A. canavarii* Checchia-Rispoli, *A. distefanoi* Checchia-Rispoli, *A. cremae* Checchia-Rispoli and *A. multicanalifera* Drobne that indicate the early-middle Cuisian (upper Ypresian, SBZ10-SBZ11). Throughout the sampled interval, we have placed the upper boundary of a composite zone called SBZ10-SBZ11 at the last occurrence of *A. schwageri*. This would be justified by the relatively wide stratigraphic range of *A. schwageri* that, even though considered as an exclusive SBZ10 marker (*A. oblonga* zone; early Cuisian) by Hottinger (1974) and Serra-Kiel et al., (1998), it is recurrently reported throughout the early-middle Cuisian (SBZ10-SBZ11) of the AdCP and Turkey as well (see Drobne, 1977; Hottinger & Drobne, 1988; Drobne & Trutin, 1997; Sirel & Acar, 2008). Full SBZ11 is characterized by the co-occurrence of *Glomalveolina* cf. *minutula* (Reichel), *A. cremae*, *A. distefanoi*, *A. multicanalifera*, *A. canavarii*, *A. decastroi* Scotto di Carlo, *A.* cf. *ruetimeyeri* Hottinger and other larger Foraminifera such as *Nummulites* sp., *Orbitolites* sp., *Ranikothalia* sp. The boundary among SBZ 11/12 is defined at the appearance of *A. rakoveci* Drobne, which is considered an endemic "Adriatic" species (Drobne et al., 2011). SBZ 12 is thus also defined by the co-occurrence with *A.* cf. *colatiensis* Drobne, *A. cremae*, *A. canavarii*, as well as nummulitids (*Nummulites* and *Operculina*), and orthophragminids in the upper section. Among the rotaliids and the other encountered lamellar perforated species, *Rotalia trochidiformis* (Lamarck), *Slovenites* sp., *Linderina* sp., *Neorotalia* cf. *litothamnica* (Uhlig), *Eponides* sp. (Fig. 9) and *Ornatorotalia spinosa* Benedetti, Di Carlo & Pignatti span through most of the section and represent a distinctive Lower-Middle Eocene assemblage with a relatively poor chronostratigraphic resolution, when compared with *Alveolina* (Benedetti et al., 2011; Hottinger, 2014). The occurrence of planktonic foraminifera identified as *Acarinina* cf. *praetopilensis* (Blow) in the uppermost portion of the section suggests an assignment to the E7-E8 plankton zones (lower Lutetian) according to the scheme of Berggren & Pearson (2005) against the GTS (Gradstein et al., 2012), which is in accordance with the data showed from the northern AdCP by Ibrahimpašić et al. (2015). This is also sustained by the chronostratigraphic recalibration made by Benedetti et al. (2023) which suggests SBZ12 extends into the lower Lutetian.

Bedding and faults assemblage

Using the software Openplot, 174 bedding attitudes and 80 planar faults segments were extracted from the 3D model (Fig. 5b). These geostructural data highlight that poles to bedding are distributed along a NE-SW direction (Fig. 10a), defining an NW-SE oriented anticline structure that is coherent with the general NE-SW shortening direction of the External Dinarides (Korbar, 2009; de Leeuw et al., 2012). The poor clustering of the poles to bedding is explained by the poor cylindricity of the fold. Data evidence that the vast majority of faults are at very high angles to bedding and with a predominant NE-SW strike (Fig. 10b). A few NE dipping reverse faults are also observed (Fig. 10b), although not along the sampled track that was in fact chosen for its apparent stratigraphic continuity. Mapped normal and strike-slip faults also seem to not impact the integrity of the sampled stratigraphic section.

Bedding planes were used to produce perpendicular-to-bedding orthoimages (here also referred to as properly oriented orthoimages) and, based on those orientations, to calculate true stratigraphic thickness between each sampling point pair. Results indicated that in the field the log was underestimated by about 14 metres, which is a 9.6% discrepancy to the total thickness (Supplement 3).

DISCUSSION

The depositional history of the Paleogene carbonate succession of the Kras-Carso, likewise those placed along the Adriatic segment of the AdCP (*sensu* Korbar, 2009), was markedly influenced by the evolving SW-verging External Dinaric orogen (see Tari, 2002; Otoničar, 2007; Korbar, 2009, and references cited herein). In accordance with the model proposed by Sabbatino et al. (2021), this succession represents the syn-orogenic deposition within the distal setting of the foredeep depozone not yet reached by the siliciclastic input. During Eocene times, these shallow-water carbonate systems stand at the final stages of their development with successive drowning - marked by the deposition of the siliciclastic units - caused by the accelerating flexural subsidence related to the development of the Dinaric fold-and-thrust belt and foreland basin system (e.g., Otoničar 2007; Korbar, 2009; Balling et al., 2021). Throughout most of the Eocene, the stratigraphic evolution of syn-orogenic shallow-water successions of the AdCP, including the Kras-Carso, was governed by the response to the migrating orogenic belt and foreland basin system at a local scale. For instance, on the Dalmatian coast of Croatia, shallow-water carbonate deposition persisted until the Bartonian (Babić & Zupanič, 2016; Ćosović et al., 2018), whereas in northern Istria it continued just up to the lower Lutetian (see e.g., Fig. 3 of Ćosović et al., 2004) until its final drowning. Mrinjek et al. (2012) suggest that these variations depend on the local timing of syndepositional tectonic deformations.

The Val Rosandra succession displays a deepening upward evolution with a facies trend that can be considered as a classical example of development and later drowning of the lower Eocene succession of the "miliolids, *Alveolina* and *Nummulites*" unit in the Kras-Carso (see also Fig. 5 of Španiček et al., 2017). It records a Ypresian to lowermost Lutetian (SBZ 10-12) shallow-water carbonate deposition ranging vertically from an inner ramp to a mid-to-outer ramp setting within the lower photic zone, and ends with lower Lutetian hemipelagic facies referable to below the photic zone, then covered by the marls of the "Transitional beds". The timing of vertical evolution constrains the drowning event of the

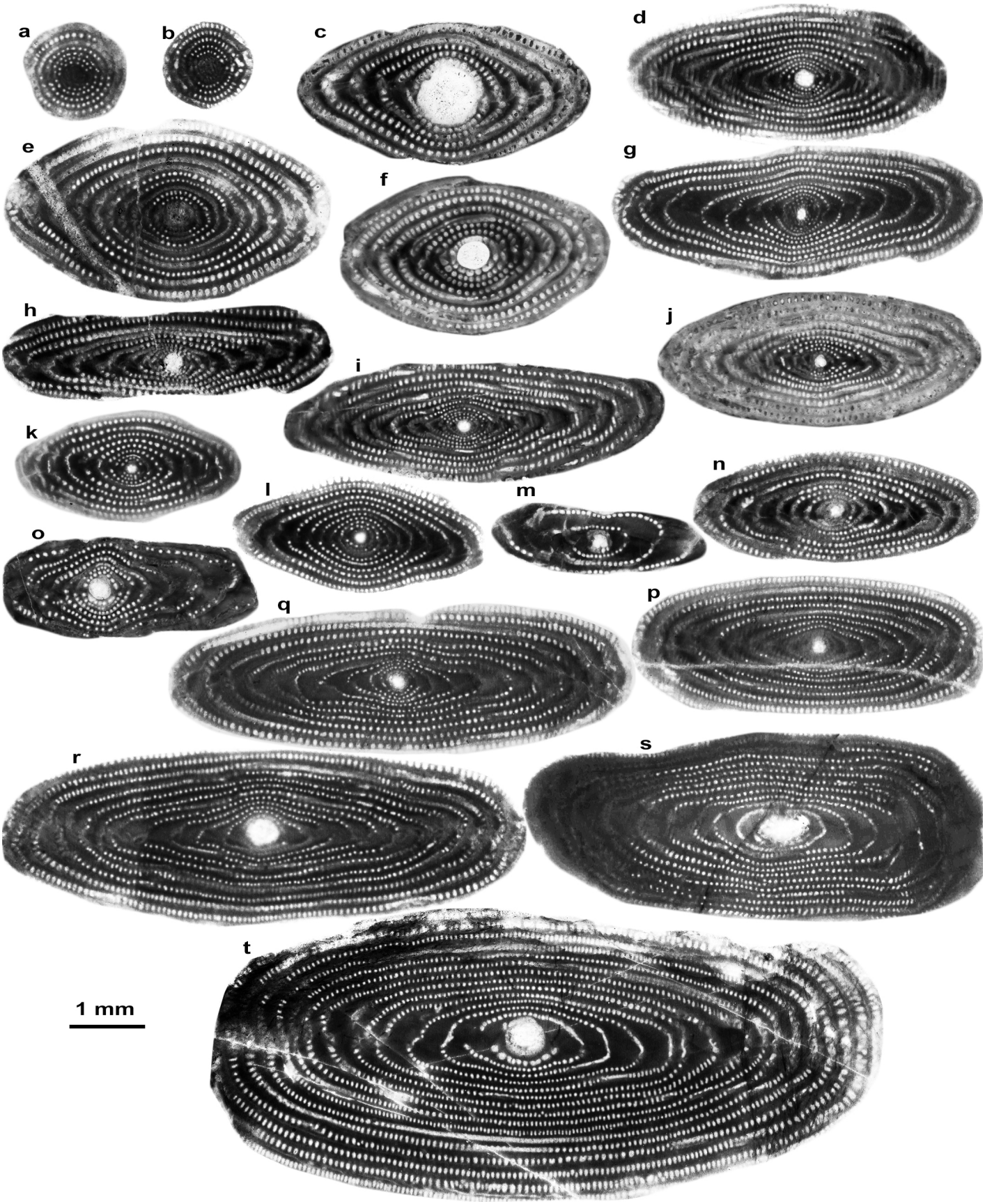

Fig. 8 - Negative pictures of *Alveolina* from polished slabs. Axial, slightly oblique centered sections of megalospheric *Alveolina* from the Val Rosandra section (Adriatic Carbonate Platform): (a, b) *Glomalveolina* cf. *minutula* (Reichel), sample VR34/1; AC11/1. (c-f) *A. cremae* Checchia-Rispoli, samples VR9; VR25; VR58, 5; AC11/2. (g-i) *A. distefanoi* Checchia-Rispoli, sample VR7/5; VR9/41; VR32/2. (j) *A. schwageri* Checchia-Rispoli, VR 33/2. (k, l) *A. decastroi* Scotto di Carlo, sample VR33/1; VR43/1. (m) *A. canavarii* Checchia-Rispoli, sample VR20/3. (n) *A.* cf. *ruetimeyeri* Hottinger, sample VR17/1. (o) *A. multicanalifera* Drobne, sample VR9/50. (p) *A.* cf. *colatiensis* Drobne, sample VR58/2. (q-r) *A. frumentiformis* Schwager, sample AC58/1-AC59/1. (s) *A. histrica histrica* Drobne, sample AC27/1; AC71/2. (t) *A. rakoveci* Drobne, sample VR50/1.

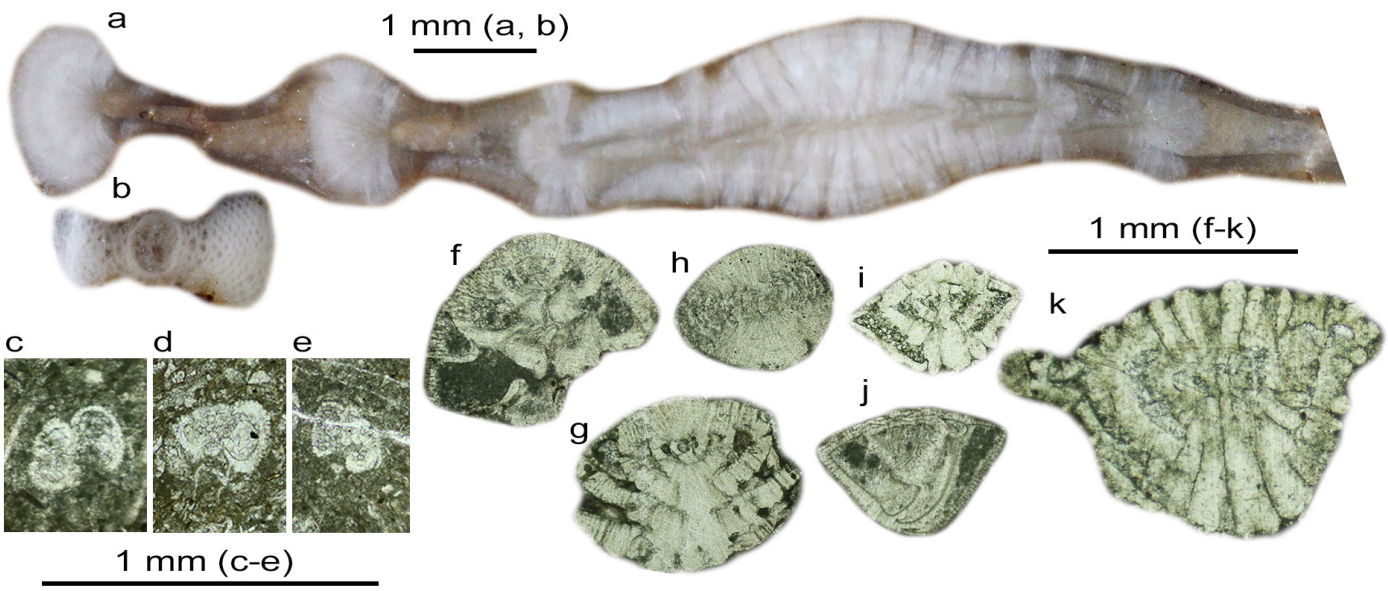

Fig. 9 - Fig. Associate foraminiferal fauna from Val Rosandra gorge - (a) *Ranikothalia* sp. polished slab, sample AC70-2. (b) *Orbitolites* sp. polished slab, sample VR42. c) Globigerinidae, sample VR61. (d, e) *Acarinina* cf. *praetopilensis*, sample VR74 and VR75. (f) *Rotalia trochidiformis*, sample VR65. (g) *Slovenites* sp. sample VR15. (h) *Linderina* sp. VR65. (i) *Neorotalia cf. litothamnica*, sample VR68. (j) *Eponides* sp. (or *Sanetschella* Ferrandez-Canadell and Baumgartner-Mora), sample VR64. (k) *Ornatorotalia spinosa*, sample VR60.

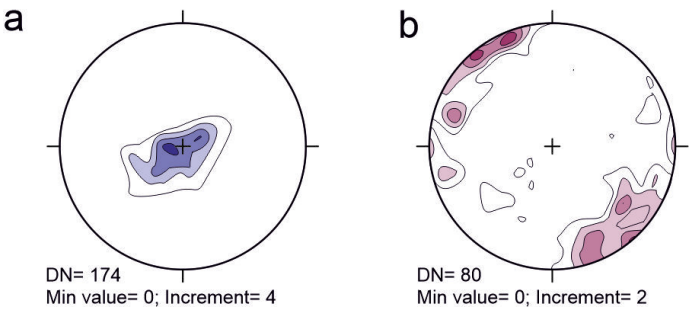

Fig. 10 - Lower hemisphere equal-area projections of cumulative density contour of poles to bedding (a) and to faults and fractures (b). DN is the data number.

carbonate factory in the studied section. This is in agreement with the data coming from northern Istria (Ćosović et al., 2004) and with previous studies made on the Val Rosandra gorge succession (Pavlovec, 1985; Drobne et al., 2009; Ibrahimpašić et al., 2015), and can be related to the large syn-tectonic influence of the Dinaric orogeny. Unlike the aforementioned works, however, the model derived from our biostratigraphic study at Val Rosandra slightly rejuvenates the age of the upper portion of platform deposits therefore postponing the drowning event in the area. This is supported by the chronostratigraphic recalibration of Benedetti et al. (2023) on SBZ12 and the occurrence of E7-E8 biozonal elements, which suggest that the upper part of the Val Rosandra succession can be fairly placed, at least, into the lowermost Lutetian. The demise of the carbonate factory is marked by the marls belonging to the "Transitional beds'' - also called in some areas "*Globigerina* marls" - which have been dated, nearby Val Rosandra, as early to middle Lutetian, within the NP15/16 biozones (Pavšič & Peckmann, 1996). The siliciclastic deposition recorded by the "Trieste flysch" has been dated as early to middle Lutetian, as within the NP14/16 biozones (Bensi et al., 2007; Cucchi & Piano, 2013).

The visual support received during the fieldwork effectively improved the rock sampling activities, including the precise geotagging of sample positions. Contextually, the collection of a tagged photographic dataset of the section enabled the application of structure from motion–multiview stereo digital photogrammetry for generating a virtual outcrop model in support of this biostratigraphic investigation. The virtual outcrop model was particularly useful to recalculate the true stratigraphic thicknesses. In fact, even though thicknesses were thoroughly measured in the field using a metre tape, discrepancies with stratigraphic thicknesses estimated from the 3D model were found (Fig. 7). 132-metre-thick log results from field measurements whereas a section thickness of 146 metres is calculated from the oriented orthoimages. Such 9.6% total difference is not negligible and may have significant impact in estimating sedimentological parameters such as sedimentation rates. The reasons of this discrepancies can be found in the working conditions. Some parts of the section were particularly difficult to walk, and sometimes the closeness to the outcrop hindered the recognition of the bedding attitude that changes along the section due to a different structural position with respect to the mapped fold (Fig. 5b). Comparison of hand-measured log and 3D model-derived log also highlights major changes in the vertical distribution of samples between samples VR35 and VR43 (Fig. 7), as well as an evident stratigraphic thickness discrepancy between the samples VR60 and VR61, where strata are affected by a major tilting. It is worth mentioning that the observed discrepancies only affected the thickness of strata while the virtual outcrop model analysis did not evidence any structural change such as in the stratigraphic

polarity. Moreover, the occurrence of the discontinuities mapped along the virtual outcrop model of the exposure (i.e., fractures and faults in figure 5b) can be considered a minor disturbance in the stratigraphic continuity of the section.

The outcrop studied in this work belongs to the sheet n.110 (Trieste) of the geological map of Italy at 1:50,000 scale, realized in the frame of the CARG geological mapping project. As a final remark, we would like to point out that, the presented case history may represent an interesting concept for data collection and integration in the CARG geodatabase (see e.g., Battaglini et al., 2022). For instance, each sample feature, including its coordinates, lithology, palaeontological content, and stratigraphic placement is directly linked to the 3D model. The model, which is already made available online, can possibly be included in official databases (e.g., the CARG database) so that all data gathered from it will be made officially available to the public. It is worth pointing out, however, that even though sharing of 3D models can be viewed as positive for the public, the routine inclusion of virtual outcrop models in cartography projects similar to CARG, would require the definition of standardized workflows to guarantee proper quality standards. This could be achieved by issuing shared guidelines to be included in official databases (e.g., Buckley et al., 2022). In addition, virtual outcrop models are a very effective way to document and preserve outcrops (Burnham et al., 2022; Corradetti et al., 2022), which could be modified or even destroyed by natural or anthropic causes and therefore hold great potential for geological cultural heritage preservation and geoscience in general. Moreover, virtual outcrop models represent the milieus for augmented accessibility, inclusivity, and scientific reproducibility (Burnham et al., 2022; Cawood et al., 2022) as well as to deliver virtual field trips (Cliffe, 2017; Pugsley et al., 2022).

CONCLUSION

The stratigraphic distribution of the larger Foraminifera, and secondarily planktonic foraminifera, recognized in the Val Rosandra gorge have allowed for dating the Eocene shallow-water succession of the "miliolids, *Alveolina* and *Nummulites* limestone" unit (of the geological sheet n. 110 Trieste) in detail. The vertical evolution of facies displays a deepening upward trend throughout the upper Ypresian-lower Lutetian, with a final demise of the carbonate factory that is consistent with the advance of the foreland basin of the Dinaric orogen front. Field activities such as sampling and measurement of the stratigraphic section were supported by the use of a drone and virtual outcrop modeling. This has permitted us to (i) place with a precision never attained each sample on its own sampling point, along the stratigraphic succession and on each sampled limestone bed; (ii) control the biases given by the hand measurements of beds through walking survey against their relative thickness corrected by using oriented orthoimages; (iii) produce a consistent 3D model for the studied outcrop. Results coming from this survey may provide a useful concept to be further explored for enhancement of the CARG database with additional digital information that could be provided by the routine application of virtual outcrop modeling in the study of stratigraphic sections.

ELECTRONIC SUPPLEMENTARY MATERIAL

This article contains electronic supplementary material which is available to authorised users.

ACKNOWLEDGEMENTS

Suggestions and personal communications on the stratigraphy and micropaleontology of the Val Rosandra area given by Katica Drobne (Lubiana), Johannes Pignatti (Rome) and Cesare Papazzoni (Modena) are warmly acknowledged. This research has been supported by fundings coming from the CARG Project – Geological Map of Italy at 1:50,000 scale. Three anonymous reviewers and the Guest Editor of the present special volume Chiara Zuffetti are thanked for thoughtful, positive, and thorough reviews that improved this paper.

REFERENCES

Accordi G., Carbone F. & Pignatti J. (1998) - Depositional history of a Paleogene carbonate ramp (western Cephalonia, Ionian Islands, Greece). Geol. Romana, 34, 131-205.

Arbués P., García-Sellés D., Granado P., López-Blanco M. & Muñoz J.A. (2012, June 4) - A Method for Producing Photorealistic Digital Outcrop Models. 74th EAGE Conference & Exhibition, http://www.earthdoc.org/publication/publicationdetails/?publication=59010.

Babić L. & Zupanič J. (2016) - The youngest stage in the evolution of the Dinaric carbonate platform: The Upper Nummulitic Limestones in the North Dalmatian foreland, Middle Eocene, Croatia. Nat. Croat., 25(1), 55-71.

Balling P., Tomljenović B., Schmid S.M. & Ustaszewski K. (2021) - Contrasting along-strike deformation styles in the central external Dinarides assessed by balanced cross-sections: Implications for the tectonic evolution of its Paleogene flexural foreland basin system. Global Planet. Change, 103587, https://doi.org/10.1016/j.gloplacha.2021.103587.

Battaglini L., Carta R., Cipriani A., Consorti L., D'Ambrogi C., Di Manna P., D'Orefice M., Falcetti, S., Fiorentin, A., Fiorenz, D., Lettieri M., Lo Faro S., Martarelli L., Muraro C., Orefice S., Papasodaro F., Pieruccioni D., Radeff G., Silvestri S., Simonetti M., Troccoli A. & Vita L. (2022) - Aggiornamento e Integrazioni delle Linee Guida per la Realizzazione della Carta Geologica d'Italia alla scala 1:50.000 Progetto Carg. (Periodici tecnici) I Quaderni, serie III, vol. 15, del Servizio Geologico d'Italia, ISPRA, Roma, 197 p., https://progetto-carg.isprambiente.it/quaderno15&oggettidigitali/Quaderno_N_15.pdf.

Bemis S.P., Micklethwaite S., Turner D., James M.R., Akciz S., Thiele S.T. & Bangash H.A. (2014) - Ground-based and UAV-Based photogrammetry: A multi-scale, high-resolution mapping tool for structural geology and paleoseismology. J. Struct. Geol., 69, 163-178, https://doi.org/10.1016/j.jsg.2014.10.007.

Benedetti A. & Papazzoni C.A. (2022) - Rise and fall of rotaliid foraminifera across the Paleocene and Eocene times. Micropaleontology, 68(2), 185-196, https://doi.org/10.47894/mpal.68.2.02.

Benedetti A., Di Carlo M. & Pignatti J. (2011) - New late Ypresian (Cuisian) rotaliids (foraminiferida) from central and southern Italy and their biostratigraphic potential. Turk. J. Earth Sci., 20(6), 701-719, https://doi.org/10.3906/yer-0910-47.

Benedetti A., Papazzoni C.A., Bosellini F., Giusberti L. & Fornaciari E. (2023) - High-diversity larger foraminiferal assemblages calibrated with calcareous nannoplankton biozones in the aftermath of EECO (Collio, Friuli-Venezia Giulia, northeastern Italy). Palaeoworld, https://doi.org/10.1016/j.palwor.2023.01.013.

Bensi S., Fanucci F., Pavšic J., Tunis G. & Cucchi F. (2007) - Nuovi dati biostratigrafici, sedimentologici e tettonici sul Flysch di Trieste. Rend. Online Soc. Geol. It., 4, 1-145.

Berggren W.A. & Pearson P.N. (2005) - A revised tropical to subtropical Paleogene planktonic foraminiferal zonation. J. Foramin. Res., 35(4), 279-298, https://doi.org/10.2113/35.4.279.

Brodu N. & Lague D. (2012) - 3D terrestrial lidar data classification of complex natural scenes using a multi-scale dimensionality criterion: Applications in geomorphology. ISPRS J. Photogramm. Remote Sens., 68, 121-134.

Buckley S.J., Howell J.A., Naumann N., Lewis C., Chmielewska M., Ringdal K., Vanbiervliet J., Tong B., Mulelid-Tynes O.S., Foster D., Maxwell G. & Pugsley J. (2022) - V3Geo: A cloud-based repository for virtual 3D models in geoscience. Geosci. Comm., 5(1), 67-82. https://doi.org/10.5194/gc-5-67-2022

Buckley S.J., Ringdal K., Naumann N., Dolva B., Kurz T.H., Howell J. A. & Dewez T.J.B. (2019) - LIME: Software for 3-D visualization, interpretation, and communication of virtual geoscience models. Geosphere, 15(1), 222–235. https://doi.org/10.1130/GES02002.1

Burnham B., Bond C., Flaig P., van der Kolk D. & Hodgetts D. (2022) - Outcrop conservation: Promoting accessibility, inclusivity, and reproducibility through digital preservation. The Sediment. Record, 20(1), 5-14. https://doi.org/10.2110/sedred.2022.1.2

Briguglio A., Giraldo-Gómez V. M., Baucon A., Benedetti A., Papazzoni C. A., Pignatti J., Wolfgring E. & Piazza M. (2023) - A middle Eocene shallow-water drowning ramp in NW Italy: from shoreface conglomerates to distal marls. Newsl. Stratigr., https://doi.org/10.1127/nos/2023/0784.

Camanni G., Vinci F., Tavani S., Ferrandino V., Mazzoli S., Corradetti A., Parente M. & Iannace A. (2021) - Fracture density variations within a reservoir-scale normal fault zone: a case study from shallow-water carbonates of southern Italy. J. Struct. Geol., 151, 104432, https://doi.org/10.1016/j.jsg.2021.104432.

Carrivick J.L. & Smith M.W. (2019) - Fluvial and aquatic applications of Structure from Motion photogrammetry and unmanned aerial vehicle/drone technology. WIREs Water, 6(1), 1-17, https://doi.org/10.1002/wat2.1328.

Carrivick J.L., Smith M.W. & Quincey D.J. (2016) - Structure from Motion in the Geosciences. Collection of New Analytical Methods in Earth Environ. Sci., https://10.1002/9781118895818.

Cawood A.J., Corradetti A., Granado P. & Tavani S. (2022) - Detailed structural analysis of digital outcrops: A learning example from the Kermanshah-Qulqula radiolarite basin, Zagros Belt, Iran. J. Struct. Geol., 154, 104489, https://doi.org/10.1016/j.jsg.2021.104489

Cliffe A.D. (2017) - A review of the benefits and drawbacks to virtual field guides in today's Geoscience higher education environment. Int. J. Educ. Technol. in Higher Educ., 14(1), https://doi.org/10.1186/s41239-017-0066-x.

Consorti L., Arbulla D., Bonini L., Fabbi S., Fanti F., Franceschi M., Frijia G. & Pini G.A. (2021) - The Mesozoic palaeoenvironmental richness of the Trieste Karst. Geological Field Trips & Maps, 13(2.2), 1-40, https://dx.doi.org/10.3301/GFT.2021.06.

Corradetti A., Seers T., Mercuri M., Calligaris C., Busetti A. & Zini L. (2022) - Benchmarking different SfM-MVS photogrammetric and iOS LiDAR acquisition methods for the digital preservation of a short-lived excavation: a case study from an area of sinkhole related subsidence. Remote Sens., 14(20), 5187, https://doi.org/10.3390/rs14205187.

Corradetti A., Tavani S., Russo M., Arbués P.C. & Granado P. (2017) - Quantitative analysis of folds by means of orthorectified photogrammetric 3D models: a case study from Mt. Catria, Northern Apennines, Italy. The Photogramm. Record, 32(160), 480-496, https://doi.org/10.1111/phor.12212.

Ćosović V., Drobne K. & Moro A. (2004) - Paleoenvironmental model for Eocene foraminiferal limestones of the Adriatic carbonate platform (Istrian Peninsula). Facies, 50, 61-75, https://doi.org/10.1007/s10347-004-0006-9.

Ćosović V., Mrinjek E., Nemec W., Španiček J. & Terzić K. (2018) - Development of transient carbonate ramps in an evolving foreland basin. Basin Res., 30(4), 746-765, https://doi.org/10.1111/bre.12274.

Cucchi F., Radrizzani C.P. & Pugliese N. (1987) - The carbonate stratigraphic sequence of the Karst of Trieste (Italy). Memorie Della Società Geologica Italiana 40. Proceedings of the International Symposium on Evolution of the Karstic Carbonate Platform, Trieste, Italy, June 1-6, 1987, 155-161.

Cucchi F. & Piano C. (2013) - Brevi note illustrative della carta geologica del Carso Classico Italiano. Progetto GEO-CGT-Cartografia Geologica Di Sintesi in Scala, 1(10.000). https://www.regione.fvg.it/rafvg/export/sites/default/RAFVG/ambiente-territorio/geologia/FOGLIA05/allegati/Note_illustrative_Carta_geologica_del_Carso_Classico.pdf

de Leeuw A., Mandic O., Krijgsman W., Kuiper K., & Hrvatović H. (2012) - Paleomagnetic and geochronologic constraints on the geodynamic evolution of the Central Dinarides. Tectonophysics, 530, 286-298, https://doi.org/10.1016/j.tecto.2012.01.004.

Devoto S., Macovaz V., Mantovani M., Soldati M. & Furlani S. (2020) - Advantages of using UAV digital photogrammetry in the study of slow-moving coastal landslides. Remote Sensing, 12(21), 3566, https://doi.org/10.3390/rs12213566.

Drobne K. (1977) - Alvéolines paléogènes de l'Istrie et de la Slovénie. Mém. Suiss. Paléontol., 99, 1-175.

Drobne K. & Trutin M. (1997) - Alveolinas from the Bunić section (Lika, Croatia). Geol. Croat., 50(2), 215-223.

Drobne K., Ogorelec B., Pavšič J. & Pavlovec R. (2009) - Paleocene and Eocene in South-western Slovenia. In: M. Pleničar, B. Ogorelec, & M. Novak (Eds.), Geology of Slovenia (pp. 311-372). Geološki zavod Slovenije.

Drobne K., Ćosović V., Moro A. & Bucković D. (2011) - The Role of the Palaeogene Adriatic Carbonate Platform in the Spatial Distribution of Alveolinids. Turk. J. Earth Sci., 20(6), 721-751, https://doi.org/10.3906/yer-0911-76.

Drobne K., Jež J., Ćosović V., Ogorelec B., Stenni B., Zakrevskaya E. & Hottinger L. (2014) - Identification of the Palaeocene–Eocene Boundary based on larger foraminifers in deposits of the Palaeogene Adriatic Carbonate Platform, southwestern Slovenia, *in* R. Rocha, J. Pais, J.C. Kullberg, and S. Finney (eds.), Strati 2013, First International Congress on Stratigraphy, At the Cutting Edge of Stratigraphy: Springer International Publishing, Stuttgart, p. 89–93. Fabuel-Perez, I., Hodgetts, D. & Redfern, J. (2010). Integration of digital outcrop models (DOMs) and high resolution sedimentology – workflow and implications for geological modeling: Oukaimeden Sandstone Formation, High Atlas (Morocco). Petrol. Geosci., 16(2), 133-154, https://doi.org/10.1144/1354-079309-820.

Favalli M., Fornaciai A., Isola I., Tarquini S. & Nannipieri L. (2012) - Multiview 3D reconstruction in geosciences. Comput. Geosci., 44, 168-176, https://doi.org/10.1016/j.cageo.2011.09.012.

Fernández O. (2005) - Obtaining a best fitting plane through 3D georeferenced data. J. Struct. Geol., 27(5), 855-858, https://doi.org/10.1016/j.jsg.2004.12.004.

Fernández O., Jones S., Armstrong N., Johnson G., Ravaglia A. & Muñoz J.A. (2009) - Automated tools within workflows for 3D structural construction from surface and subsurface data. GeoInformatica, 13(3), 291-304, https://doi.org/10.1007/s10707-008-0059-y.

Furlani S., Bolla A., Hastewell L., Mantovani M. & Devoto S. (2022) - Integrated Geomechanical and Digital Photogrammetric Survey in the Study of Slope Instability Processes of a Flysch Sea Cliff (Debeli Rtič Promontory, Slovenia). Land, 11(12). https://doi.org/10.3390/land11122255

Franceschi M., Martinelli M., Gislimberti L., Rizzi A. & Massironi M. (2015) - Integration of 3D modeling, aerial LiDAR and photogrammetry to study a synsedimentary structure in the Early Jurassic Calcari Grigi (Southern Alps, Italy). Eur. J. Remote Sens., 48, 527-539, https://doi.org/10.5721/EuJRS20154830.

Gradstein F.M., Ogg J. G., Schmitz M. & Ogg G. (Eds.). (2012) - The geologic time scale 2012. Elsevier.

Hohenegger J. (2000) - Coenoclines of larger foraminifera. Micropaleontology, 46, 127-151, https://www.jstor.org/stable/1486185.

Hottinger L. (1974) - Alveolinids, Cretaceous-Tertiary larger foraminifera. Exxon Production Research Company, Technical Information Services.

Hottinger L. (1997) - Shallow benthic foraminiferal assemblages as signals for depth of their deposition and their limitations. Bull. Soc. géol. Fr., 168(4), 491-505.

Hottinger L. (2001) - Learning from the past. In R. Levi-Montalcini (ed.): Frontiers of Life 4(2): Discovery and spoliation of the biosphere (pp. 449-477). Academic Press.

Hottinger L. (2014) - Paleogene larger rotaliid foraminifera from the western and central Neotethys (D. Bassi (ed.)). Springer International Publishing, https://doi.org/10.1007/978-3-319-02853-8.

Hottinger L. & Drobne K. (1988) - Alvéolines tertiaires: quelques problèmes liés à la conception de l'espèce. Rev. Paléobiol., 2, 665-685.

Hottinger L., Hedley R. H. & Adams G. (1978) - Comparative anatomy of selected foraminiferal shell structures. In: T. B. F. Harding & J. A. R. Riedel (Eds.), Foraminifera III (pp. 203-266). Academic Press.

Ibrahimpašić H., Premec Fućek V., Hernitz Kučenjak M., Drobne K., Celarc B. & Placer L. (2015) - Paleogene NW Adria block surrounded by deeper basins; study by plankton, small and larger foraminifera on the drowning time in Late Ilerdian, Late Cuisian and Middle Lutetian (N Italy, SW Slovenia, SW Croatia – Istria, Kvarner). 2nd International Congress on Stratigraphy, STRATI 2015, 172.

Jablonska D., Pitts A., Di Celma C., Volatili T., Alsop G.I. & Tondi E. (2021) - 3D outcrop modeling of large discordant breccia bodies in basinal carbonates of the Apulian margin, Italy. Marine and Petroleum Geology, 123(June 2020), 104732. https://doi.org/10.1016/j.marpetgeo.2020.104732

James M.R. & Robson S. (2012) - Straightforward reconstruction of 3D surfaces and topography with a camera: Accuracy and geoscience application. J. Geophys. Res., 117(F3), F03017, https://doi.org/10.1029/2011JF002289.

Jones R.R., Pearce M.A., Jacquemyn C. & Watson F.E. (2016) - Robust best-fit planes from geospatial data. Geosphere, 12(1), 196-202, https://doi.org/10.1130/GES01247.1.

Jurkovšek B., Biolchi S., Furlani S., Kolar-Jurkovšek T., Zini L., Jež J., Tunis G., Bavec M. & Cucchi F. (2016) - Geology of the classical karst region (SW Slovenia–NE Italy). J. Maps, 12(sup1), 352-362, https://doi.org/10.1080/17445647.2016.1215941.

Korbar T. (2009) - Orogenic evolution of the External Dinarides in the NE Adriatic region: a model constrained by tectonostratigraphy of Upper Cretaceous to Paleogene carbonates. Earth-Sci. Rev., 96(4), 296-312, https://doi.org/10.1016/j.earscirev.2009.07.004.

Leutenegger S. (1984) - Symbiosis in benthic foraminifera; specificity and host adaptations. J. Foramin. Res., 14(1), 16-35, https://doi.org/10.2113/gsjfr.14.1.16.

Mammoliti E., Pepi A., Fronzi D., Morelli S., Volatili T., Tazioli A. & Francioni M. (2023) - 3D Discrete Fracture Network Modelling from UAV Imagery Coupled with Tracer Tests to Assess Fracture Conductivity in an Unstable Rock Slope: Implications for Rockfall Phenomena. Remote Sens., 15(5), https://doi.org/10.3390/rs15051222.

Manniello C., Abdallah I.B., Prosser G. & Agosta F. (2023) - Pressure solution-assisted diagenesis and thrusting-related deformation of Mesozoic platform carbonates. J. Struct. Geol., 173, 104906, https://doi.org/10.1016/j.jsg.2023.104906.

Marques A., Horota R.K., de Souza E. M., Lupssinskü L., Rossa P., Aires A.S., Bachi L., Veronez M.R., Gonzaga L. & Cazarin C.L. (2020) - Virtual and digital outcrops in the petroleum industry: A systematic review. Earth-Sci. Rev., 208(September 2019), 103260, https://doi.org/10.1016/j.earscirev.2020.103260.

Menegoni N., Giordan D., Perotti C. & Dwayne D. (2019) - Detection and geometric characterization of rock mass discontinuities using a 3D high-resolution digital outcrop model generated from RPAS imagery - Ormea rock slope, Italy. Eng. Geol., 252, 145-163, https://doi.org/10.1016/j.enggeo.2019.02.028.

Menegoni N., Meisina C., Perotti C. & Crozi M. (2018) - Analysis by UAV digital photogrammetry of folds and related fractures in the monte antola flysch formation (Ponte organasco, Italy). Geosciences, 8, https://doi.org/10.3390/geosciences8080299

Mrinjek E., Nemec W., Pecinger V., Mikša G., Vlahović I., Ćosović V., Velić I., Bergant S. & Matičec D. (2012) - The Eocene-Oligocene Promina Beds of the Dinaric Foreland Basin in Northern Dalmatia. J. Alpine Geol., 55, 409-451.

Nesbit P.R., Durkin P.R., Hugenholtz C.H., Hubbard S.M. & Kucharczyk M. (2018) - 3-D stratigraphic mapping using a digital outcrop model derived from UAV images and structure-from-motion photogrammetry. Geosphere, 14(6), 2469-2486, https://doi.org/10.1130/GES01688.1.

Otoničar B. (2007) - Upper Cretaceous to Paleogene forbulge unconformity associated with foreland basin evolution (Kras, Matarsko Podolje and Istria; SW Slovenia and NW Croatia). Acta Carsologica, 36(1), https://doi.org/10.3986/ac.v36i1.213.

Panara Y., Menegoni N., Carboni F. & Inama R. (2022) - 3D digital outcrop model-based analysis of fracture network along the seismogenic Mt. Vettore Fault System (Central Italy): the importance of inherited fractures. J. Struct. Geol., 161, https://doi.org/10.1016/j.jsg.2022.104654.

Papazzoni C.A., Fornaciari B., Giusberti L., Simonato M. & Fornaciari E. (2023) - A new definition of the Paleocene Shallow Benthic Zones (SBP) by means of larger foraminiferal biohorizons, and their calibration with calcareous nannofossil biostratigraphy. Micropaleontology, 69, 363-400.

Pavlovec R. (1985) - Numulitine iz apnencev pri Izoli (SW Slovenija): Nummulitines from limestones at Izola (Istria, W Yugoslavia) Razprave 4. razr. SAZU, 26, 219-230..

Pavšič J. & Peckmann J. (1996) - Stratigraphy and sedimentology of the Piran flysch area (Slovenia). Annales, 9, 123-138.

Pignatti J.S. (1995) - Biostratigrafia dei macroforaminiferi del Paleogene della Maiella nel quadro delle piattaforme periadriatiche. In: Mancinelli A. (Ed.), Biostratigrafia dell'Italia centrale. Studi Geologici Camerti, Volume Speciale, 1994, 359-405. Camerino.

Pignatti J. & Papazzoni C.A. (2017) - Oppelzones and their heritage in current larger foraminiferal biostratigraphy. Lethaia, 50(3), 369-380, https://doi.org/10.1111/let.12210.

Pugsley J.H., Howell J.A., Hartley A., Buckley S.J., Brackenridge R., Schofield N., Maxwell G., Chmielewska M., Ringdal K., Naumann N. & Vanbiervliet J. (2022) - Virtual field trips utilizing virtual outcrop: construction, delivery and implications for the future. Geosci. Comm., 5(3), 227-249, https://doi.org/10.5194/gc-5-227-2022.

Romero J., Caus E. & Rosell J. (2002) - A model for the palaeoenvironmental distribution of larger foraminifera based on late Middle Eocene deposits on the margin of the South Pyrenean basin (NE Spain). Palaeogeogr., Palaeocl., 179(1-2), 43-56, https://doi.org/10.1016/S0031-0182(01)00406-0.

Sabbatino M., Tavani S., Vitale S., Ogata K., Corradetti A., Consorti L., Arienzo I., Cipriani A. & Parente M. (2021) - Forebulge migration in the foreland basin system of the central-southern Apennine fold-thrust belt (Italy): New high-resolution Sr-isotope dating constraints. Basin Research, November 2020, bre.12587, https://doi.org/10.1111/bre.12587.

Scheibner C. & Speijer R.P. (2008) - Late Paleocene–early Eocene Tethyan carbonate platform evolution—A response to long-and short-term paleoclimatic change. Earth-Sci. Rev., 90(3-4), 71-102, https://doi.org/10.1016/j.earscirev.2008.07.002.

Schilirò L., Robiati C., Smeraglia L., Vinci F., Iannace A., Parente M. & Tavani S. (2022) - An integrated approach for the reconstruction of rockfall scenarios from UAV and satellite-based data in the Sorrento Peninsula (southern Italy). Eng. Geol., 308, https://doi.org/10.1016/j.enggeo.2022.106795.

Schmid S.M., Bernoulli D., Fügenschuh B., Matenco L., Schefer S., Schuster R., Tischler M. & Ustaszewski K. (2008) - The Alpine-Carpathian-Dinaridic orogenic system: correlation and evolution of tectonic units. Swiss J. Geosci., 101, 139-183, https://doi.org/10.1007/s00015-008-1247-3.

Seers T.D. & Hodgetts D. (2016) - Probabilistic constraints on structural lineament best fit plane precision obtained through numerical analysis. J. Struct. Geol., 82, 37-47, https://doi.org/10.1016/j.jsg.2015.11.004.

Seers T.D., Sheharyar A., Tavani S. & Corradetti A. (2021) - Virtual outcrop geology comes of age: The application of consumer-grade virtual reality hardware and software to digital outcrop data analysis. Computers & Geosciences, 105006, https://doi.org/10.1016/j.cageo.2021.105006.

Serra-Kiel J., Hottinger L., Caus E., Drobne K., Ferrandez C., Jauhri A. K., Less G., Pavlovec R., Pignatti J., Samso J.M., Schaub H. Sirel E., Strougo A., Tambareau Y., Tosquella J. & Zakrevskaya E. (1998) - Larger foraminiferal biostratigraphy of the Tethyan Paleocene and Eocene. Bull. Soc. Géol. Fr., 169(2), 281-299.

Sinanoğlu D., Benedetti A. & Özgen-Erdem N. (2022) - Danian (SBZ2) Larger Foraminifera from the Becirman Formation (Southeastern Turkey) as Evidence of Rotaliids Diversity In Lower Paleocene Shallow-Water Environments. Riv. Ital. Paleontol. S., 128(2), 431-452.

Sirel E. & Acar Ş. (2008) - Description and biostratigraphy of the Thanetian-Bartonian Glomalveolinids and Alveolinids of Turkey. TMMOB Jeoloji Mühendisleri Odası.

Španiček J., Ćosović V., Mrinjek E. & Vlahović I. (2017) - Early Eocene evolution of carbonate depositional environments recorded in the Čikola canyon (north Dalmatian Foreland Basin, Croatia). Geol. Croat., 70(1), 11-25, https://doi.org/10.4154/gc.2017.05.

Tari Kovačić V. & Mrinjek E. (1994) - The role of Palaeogene clastics in the tectonic interpretation of Northern Dalmatia (Southern Croatia) Geol. Croat., 47/1, 127-138, https://doi.org/10.4154/GC.1994.10.

Tari V. (2002) - Evolution of the northern and western Dinarides: a tectonostratigraphic approach. EGU Stephan Mueller Special Publication Series, 1, 223-236.

Tavani S., Arbues P., Snidero M., Carrera N. & Muñoz J.A. (2011) - Open Plot Project: an open-source toolkit for 3-D structural data analysis. Solid Earth, 2(1), 53-63, https://doi.org/10.5194/se-2-53-2011.

Tavani S., Corradetti A. & Billi A. (2016) - High precision analysis of an embryonic extensional fault-related fold using 3D orthorectified virtual outcrops: The viewpoint importance in structural geology. J. Struct. Geol., 86, 200-210, https://doi.org/10.1016/j.jsg.2016.03.009.

Tavani S., Granado P., Corradetti A., Girundo M., Iannace A., Arbués P., Muñoz J.A. & Mazzoli S. (2014) - Building a virtual outcrop, extracting geological information from it, and sharing the results in Google Earth via OpenPlot and Photoscan: An example from the Khaviz Anticline (Iran). Comput. Geosci., 63, 44-53, https://doi.org/10.1016/j.cageo.2013.10.013.

Tavani S., Ogata K., Vinci F., Sabbatino M., Kylander-Clark A., Caterino G., Buglione A., Cibelli A., Maresca A., Iacopini D., Parente M. & Iannace A. (2023) - Post-rift Aptian-Cenomanian extension in Adria, insight from the km-scale Positano-Vico Equense syn-sedimentary fault. J. Struct. Geol., 168, 104820, https://doi.org/10.1016/j.jsg.2023.104820.

van Hinsbergen D.J., Torsvik T.H., Schmid S.M., Maţenco L.C., Maffione M., Vissers R.L., Gürer D. & Spakman W. (2020) - Orogenic architecture of the Mediterranean region and kinematic reconstruction of its tectonic evolution since the Triassic. Gondwana Res., 81, 79-229, https://doi.org/10.1016/j.gr.2019.07.009.

van Unen M., Matenco L., Nader F.H., Darnault R., Mandic O. & Demir V. (2019) - Kinematics of foreland-vergent crustal accretion: Inferences from the Dinarides evolution. Tectonics, 38(1), 49-76, https://doi.org/10.1029/2018TC005066.

Vecsei A., Sanders D.G.K., Bernoulli D., Eberli G.P. & Pignatti J.S. (1999) - Cretaceous to Miocene sequence stratigraphy and evolution of the Maiella carbonate platform margin, Italy. In P. C. de Graciansky, J. Hardenbol, T. Jacquin, & P. R. Vail (Eds.), Mesozoic and Cenozoic Sequence Stratigraphy of European Basins (pp. 499-512). SEPM Society for Sedimentary Geology, Special Publication, 60, https://doi.org/10.2110/pec.98.02.0053.

Verhoeven G. (2011) - Taking computer vision aloft–archaeological three-dimensional reconstructions from aerial photographs with photoscan. Archaeol. Prospect, 18(1), 67-73, https://doi.org/10.1002/arp.399.

Vlahović I., Tišljar J., Velić I. & Matičec D. (2005) - Evolution of the Adriatic Carbonate Platform: Palaeogeography, main events and depositional dynamics. Palaeogeogr., Palaeocl., 220(3-4), 333-360, https://doi.org/10.1016/j.palaeo.2005.01.011.

Zamagni J., Mutti M., Ballato P. & Košir A. (2012) - The Paleocene-Eocene thermal maximum (PETM) in shallow-marine successions of the Adriatic carbonate platform (SW Slovenia). Geol. Soc. Am. Bull., 124(7-8), 1071-1086.

Zhang Q., Willems H. & Ding L. (2013) - Evolution of the Paleocene-Early Eocene larger benthic foraminifera in the Tethyan Himalaya of Tibet, China. Int. J. Earth Sci., 102, 1427-1445, https://doi.org/10.1007/s00531-012-0856-2.